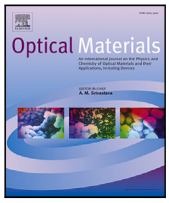
Optical Materials 157 (2024) 116334



Contents lists available at ScienceDirect

Optical Materials

journal homepage: www.elsevier.com/locate/optmat



Research article



Assembling of truncated deterministic aperiodic lattices with defects using Weber beams

Aleksandar Ž. Tomović [a], Isidora J. Vlaović Mitić [b,*], Vladimir P. Jovanović [a], Dejan V. Timotijević [a], Dragana M. Jović Savić [b]

[a] Institute for Multidisciplinary Research, University of Belgrade, Kneza Višeslava 1, 11030, Belgrade, Serbia
[b] Institute of Physics, University of Belgrade, P.O. Box 68, 11001, Belgrade, Serbia

ARTICLE INFO

MSC:
78-05
78A60
82D25

Keywords:
Weber beams
Deterministic aperiodic photonic lattice
Lattice defects

ABSTRACT

We introduce an experimental approach to realize truncated 2D deterministic aperiodic photonic structures using the interference of two mutually coherent Weber beams. The optical induction process for generating refractive index modulations in SBN crystal is controlled via various combinations of parabolic beams, with different offsets in both transverse dimensions, orientations, and relative phases, to obtain meta-structures.

1. Introduction

While light propagation in periodic (commensurable) photonic structures is controlled by photonic band gaps in space and time, and random photonic structures support light localization [1], manipulation of light by deterministic aperiodic (incommensurable) and complex photonic structures [2] at the intersection between periodic and random structures have not yet been fully understood nor exploited for applications. The discovery of quasicrystals in condensed matter [3] and their theoretical analysis [4] has inspired a new field of quasi-periodic photonic structures investigation in optics and photonics [5]. There are also plenty of examples of deterministic aperiodic structures [6] possessing different degrees of order [7]. Lebesgue's decomposition theorem was suggested to categorize structures along their spectral appearance [8,9], including Fibonacci patterns [10,11] as aperiodic structures with the highest order and low-order Rudin–Shapiro patterns [6]. Various photonic quasicrystals and deterministic aperiodic systems have been realized in optics [5,9,12–15], providing significant flexibility in engineering the optical response for applications in future devices [6,14,15].

Nondiffracting beams, with their propagation-invariant intensity distributions [16–18], facilitate the creation of photonic lattices in photosensitive media [19] and enable novel applications, particularly in optics and atom physics [20]. Optical micromanipulation technologies based on nondiffracting beams have become valuable in medical, biological, and physics research [20]. Using synthesized multiple optical beams enables much greater freedom in object manipulation [21]. We previously, theoretically and experimentally, investigated light propagation and localization in photonic structures generated by a coherent mixture of Mathieu beams in the photorefractive medium [22–24]. Parabolic (Weber) beams are nondiffracting solutions of the Helmholtz equation obtained by separation in parabolic cylindrical coordinates [18], and their uses include optically-induced lattices [19] and particle manipulation [25]. The geometrical characteristics of Weber beams offer a specific level of control over the topology of synthesized photonic structures.

Surface states, as a specific type of waves propagating along an interface separating two different media, have attracted great interest in optical systems owing to possible novel applications in all-optical switching and sensing [26,27]. The truncation of photonic lattices induces the formation of localized surface states demonstrated in 1D waveguide arrays [28,29] and 2D photonic lattices [30]. Also, the insertion of lattice defects may produce an additional physical mechanism for light confinement and possibilities of light control in photonic lattices [31–33].

In this paper, using a coherent mixture of two Weber beams, we extend the concept of 2D deterministic aperiodic lattice generation. We

* Corresponding author.
E-mail address: isidora@ipb.ac.rs (I.J. Vlaović Mitić).

https://doi.org/10.1016/j.optmat.2024.116334
Received 31 July 2024; Received in revised form 9 September 2024; Accepted 23 October 2024
Available online 30 October 2024
0925-3467/© 2024 The Author(s). Published by Elsevier B.V. This is an open access article under the CC BY-NC-ND license (http://creativecommons.org/licenses/by-nc-nd/4.0/).

superimposed two parabolic beams with different structure sizes, orientations, mutual distances, and phase relations to acquire non-diffracting intensity distributions, i.e., photonic structures (lattices) in the air. Furthermore, these generated lattices were written (optically-induced) in a single-pass experiment in photorefractive media (SBN crystal) as refractive index variations. We confirm the transverse-invariant character of lattices in SBN crystal by probing them with plane waves. Numerical simulations for predicting deterministic aperiodic lattice structure agree well with their experimental realization. Depending on the parameters of two input Weber beams, fine-tuning of resulting photonic lattice properties (shape, symmetry, defects, edges, etc.) can be achieved. In addition to being deterministic and aperiodic, Weber-beam-induced structures inscribed in the medium are ***naturally truncated***; therefore, build-up processes, such as multiplexing or occlusion, are avoided for their generation. Observed photonic lattices possess distinct regions of various shapes, transition lines, and areas with defects (dot, line shape, or macro defects) that are interesting for future investigation. The possibility of fine-tuning lattice edge shapes and strengths could be valuable in studies of surface states.

2. Generation of parabolic deterministic aperiodic lattices

The beams used for deterministic aperiodic lattice generation in this work are based on the interference of even non-diffracting Weber beams [18], mathematically described as a product of appropriate even parabolic cylinder functions P_e:

$$U_e(\eta,\xi;a)=\frac{1}{\pi\sqrt{2}}|\Gamma_1|^2 P_e(\sigma\xi;a)P_e(\sigma\eta;-a), \tag{1}$$

where $\Gamma_1 = \Gamma[(1/4)+(1/2)ia]$, $\sigma=(2k_t)^{1/2}$, $k_t=2\pi/\lambda$, and a is a parameter controlling the curvature of Weber beam lobes that we will use as a measure of parabolicity. η and ξ are parabolic cylinder coordinates and their relation with spatial Cartesian coordinates x and y is defined by transformation $x+iy=(\eta+i\xi)^2/2$.

Due to the robustness of the nondiffractive character of Weber beams in weak nonlinearity, we use them for propagation-invariant transverse intensity distributions, able to generate optically induced 2D photonic lattices. We numerically investigate conditions under which two coherently superimposed parabolic beams generate a photonic lattice that can be experimentally realized in photorefractive crystal SBN. Fig. 1(a) schematically presents our typical manipulations with basic Weber beam parameters: parabolicity and positions of focal points and their effect on the relative distance between two beams. Beam focal point positions are determined with coordinates d_x and d_y in $x-y$ plane. Weber beam orientation is defined with the sign of parabolicity, while parabolicity controls the curvature of the structure.

2.1. Theoretical model

We are modeling the generation of the deterministic aperiodic parabolic lattices using an anisotropic model consisting of a nonlinear Schrödinger-like equation as the propagation equation and the diffusion equation for the electrostatic potential as the potential equation [34,35]. The propagation equation for the scalar electric field A in the slowly varying amplitude approximation is given by:

$$i\partial_z A+\frac{1}{2k_z}\left[\Delta_\perp+V(I)\right]A=0, \tag{2}$$

where $V(I)=-k_z^2 n_{o,e}^2 r_{13,33}E(E_{sc})$ is nonlinear potential defined by the photorefractive nonlinearity, $n_e=2.325$ and $n_o=2.358$ are the extraordinary and ordinary indices and $r_{13}=47$ pm/V, $r_{33}=237$ pm/V are corresponding electro-optic coefficients of birefringent SBN61:Ce crystal, respectively. The electric field $E\left(E_{sc}\right)=E_{ext}+E_{sc}$ that builds up inside the crystal is a superposition of an external electric field $E_{ext}=2000$ V/cm, which is aligned along the optical $c=x$-axis and an internal space charge field (E_{sc}) that results due to the incident intensity distribution with a potential equation.

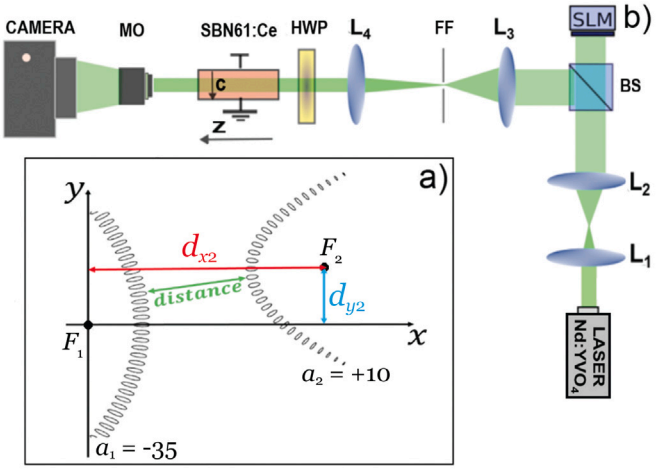


Fig. 1. (a) Illustration of basic parameters of two Weber beams: parabolicities a_1 and a_2, focal points F_1 and F_2 and their positions ($d_{x1}=0$, $d_{y1}=0$) and (d_{x2}, d_{y2}) in the $x-y$ plane. (b) The experimental setup. L - lens, BS - depolarized beam splitter, SLM - spatial light modulator, FF - Fourier filter, SBN61:Ce – medium, HWP – half-wave plate, MO - microscope objective.

To take the electric bias of the crystal into account and the photorefractive material response, we implement an anisotropic potential equation for the spatial evolution of the electrostatic potential ϕ_{sc} of the optically induced space-charge field E_{sc}

$$\Delta_\perp\phi_{sc}+\nabla_\perp\ln(1+I)\cdot\nabla_\perp\phi_{sc}=E_{ext}\partial_x\ln(1+I), \tag{3}$$

where $I=|A|^2$ is obtained from Eq. (2). Subsequently, Eq. (2) is updated with the optically induced space-charge field $E_{sc}=\partial_x\phi_{sc}$, obtained by solving Eq. (3). To solve the system of Eqs. (2) and (3) numerically, this procedure iteratively repeats along the propagation.

The process of photonic lattice generation is modeled through potential $I=I_{latt}$ (Eq. (2)), which we refer to as a writing lattice pattern in the experiment [22]. First, we obtain the spatial distribution of I_{latt} in a separate numerical simulation of Eqs. (2) and (3) propagating ordinary superimposed two Weber beams in the case of weak nonlinearity. Then, we use such obtained distribution as the lattice potential for the simulation of extraordinary Gaussian probe beam propagation using equations modified such that $I=I_p+I_{latt}$, where the Gaussian probe beam intensity $I_p=|A|^2$ is obtained from Eq. (2). In our probing simulations I_p is sufficiently weak so as not to cause nonlinear modification.

2.2. Experimental method

To experimentally investigate parabolic deterministic aperiodic photonic lattices generation, we use the experimental setup shown in Fig. 1. Our light source is a continuous frequency-doubled $Nd:YVO_4$ laser with a wavelength of $\lambda=532$ nm (Spectra Physics Millennia eV with 5 W maximum output power). Expanded and collimated by a telescope (L1-L2), the linearly polarized laser beam acts as a plane wave that illuminates a phase-only Holoeye Pluto spatial light modulator (SLM) with a resolution of 1920 × 1080 and 8 μm pixel pitch. The L1 and L2 focal lengths are 60 mm and 200 mm, respectively. The SLM modulates both the amplitude and the phase of the reflected light field. This modulation is achieved by applying a precomputed hologram to the SLM that contains information about the complex light field of two superimposed Weber beams encoded with an additional blaze grating. This process transforms an ordinary polarized beam into a spatially modulated initiation beam. That beam, demagnified using a telescope (L3-L4), illuminates a crystal. The L3 and L4 focal lengths are 400 mm and 75 mm, respectively. The diffraction pattern of the Weber lattice undergoes bandpass filtering in Fourier space (FF). The SBN61:Ce crystal (doped with $0,002\%$ CeO_2), with dimensions of

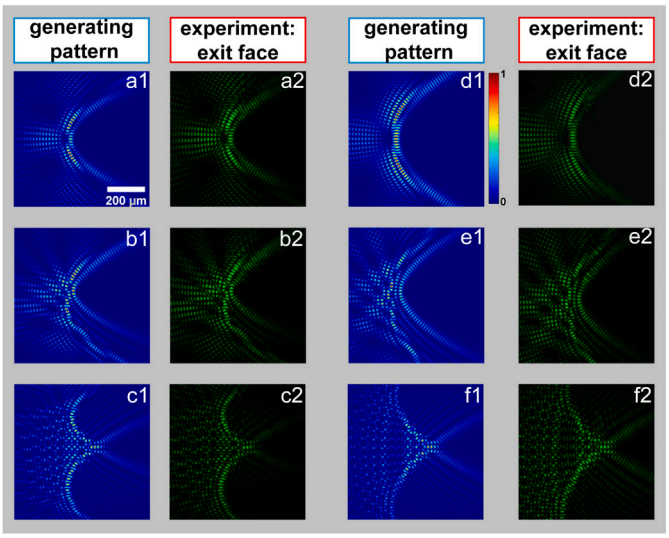


Fig. 2. Interference of two Weber beams. Transverse intensity distributions for beams of the common orientation: (a–c) $a_1 = 10$ and $a_2 = 15$ and (d–f) $a_1 = 20$ and $a_2 = 25$, with various y-axis positions: (a),(d) $d_y = 0$ μm, (b) $d_y = 108$ μm, (c) $d_y = 378$ μm, (e) $d_y = 162$ μm and (f) $d_y = 594$ μm. Input beams have the same phases (equal to 0) and x-axis positions $d_x = 0$.

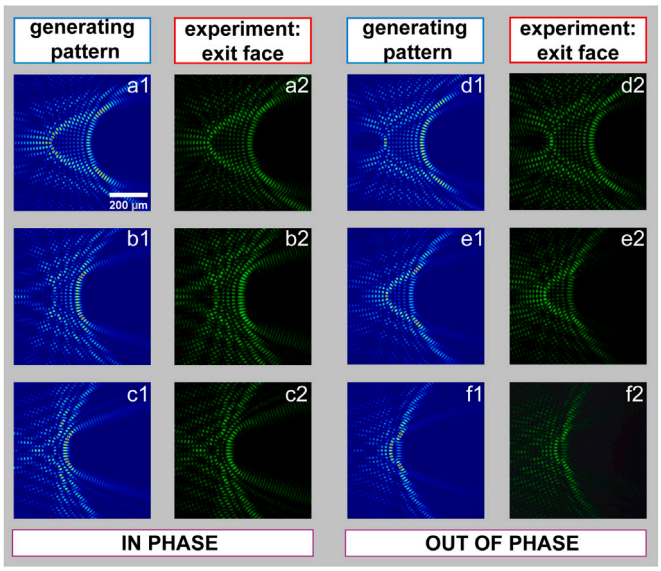


Fig. 3. Influence of horizontal beam shift and mutual phases. (a), (d) $a_1 = 5$, $a_2 = 20$, $d_x = 54$ μm, (b), (e) $a_1 = 5$, $a_2 = 30$, $d_x = 108$ μm and, (c), (f) $a_1 = 5$, $a_2 = 40$, $d_x = 162$ μm. In-phase configurations: the first and second column and out-of-phase: the third and fourth column. The y-axis position d_y is the same for all beams and is equal to 0.

5 mm × 5 mm × 20 mm, is externally biased with an electric field (E_{ext} = 2000 V/m) aligned along the optical $c = x$ axis, perpendicular to the direction of propagation (z-axis). Then, the ordinarily polarized beam (optically) induces a modulation in the refractive index by employing the lattice writing beam power ($P = 1$ mW), corresponding to the numerically calculated Weber lattice. An imaging system consisting of a 10x microscope objective (MO) with a Canon EOS 60D (with 5184 × 3456 square pixels with the pitch of 4.3 μm) camera is used to capture the transverse intensity distribution of the writing beam on the backside of the crystal. Illumination of the SBN crystal with an extraordinarily polarized broad Gaussian probe beam (linear light propagation) is used to verify the existence of the deterministic aperiodic 2D photonic lattices inscribed in the crystal.

3. Results

The first part of this section deals with combining two Weber beams to generate various shapes of deterministic aperiodic 2D photonic lattices (Figs. 2–5). All the generated photonic structures were written in the SBN crystal (the writing process generates the crystal's refraction index modulations). The fact that photographs at the input and exit sides of the crystal match implies their nondiffracting nature constant in longitudinal dimension. Experimental verification, employing the plane wave guiding technique (Fig. 6), that the superimposed Weber beams induced photonic lattices in the SBN crystal is given in the second part of this section.

3.1. Photonic lattices obtained by mixing two Weber beams

Owing to its shape, the Weber beam can be instrumental in the optical induction of semi-infinite photonic lattice with concave parabolic edge, discrete diffraction control, and surface states observation in parabolic geometry. In our investigation, the interference of two Weber beams leads to the emergence of new diffraction geometries. Two Weber beams with parabolicities a_1 and a_2 and various mutual orientations (same or opposite parabolicity sign), phases, and distances between them were used. Novel kinds of deterministic aperiodic photonic lattices with various lattice edge geometries and new types of defects were generated using such interference patterns. We demonstrate that

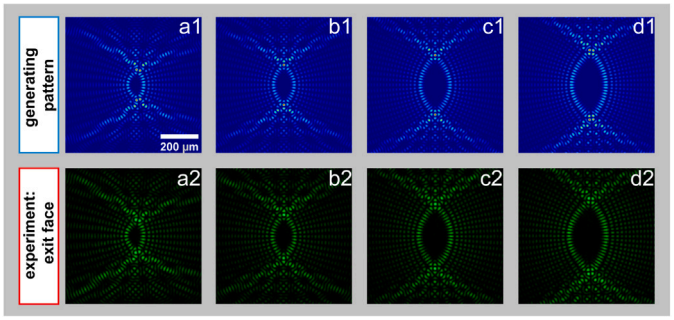


Fig. 4. Interference of two Weber beams with opposite-sing parabolicities (a) $a_1 = 5, a_2 = -10$, (b) $a_1 = 10, a_2 = -10$, (c) $a_1 = 15, a_2 = -15$ and (d) $a_1 = 15, a_2 = -20$. Input beams have the same phases, x- and y-axis positions, all equal to 0.

such superposition of two Weber beams can serve as complex aperiodic writing light capable of being transferred to tailored refractive index modulations, i.e., written in photosensitive media. In the following figures (Figs. 2–5) we present side by side view of transverse intensities of generating patterns and intensity distributions of their propagation at the exit crystal face obtained in the experiment. The longitudinal (z-direction) dimension of a nondiffracting aperiodic structure in the air is a few times larger than the one written in the SBN crystal. A comparison of images of the lattice structures monitored at the crystal input and the crystal exit sides shows that they are the same, confirming the nondiffracting lattice character within the crystal. The longitudinal dimension of structures given in Figs. 2–5 depends on the telescope L3-L4 and the structure size of the beam (lattice period): a smaller lattice period means a shorter longitudinal dimension of structures.

We start our study with two Weber beams of different positive parabolicities ($a_1, a_2 > 0$ and $a_1 \neq a_2$), for various y-axis positions (d_y) and the same x-axis positions ($d_x = 0$) (Fig. 2). The structures that are symmetric under reflection over horizontal axes are presented in Figs. 2(a) and 2(d). Sliding one of Weber beams along the y-direction breaks that symmetry, leading to intensity distributions of various asymmetries (Fig. 2(b), (c), (e), and (f)). Both combinations of parabolic beams produce truncated photonic lattices that have regions

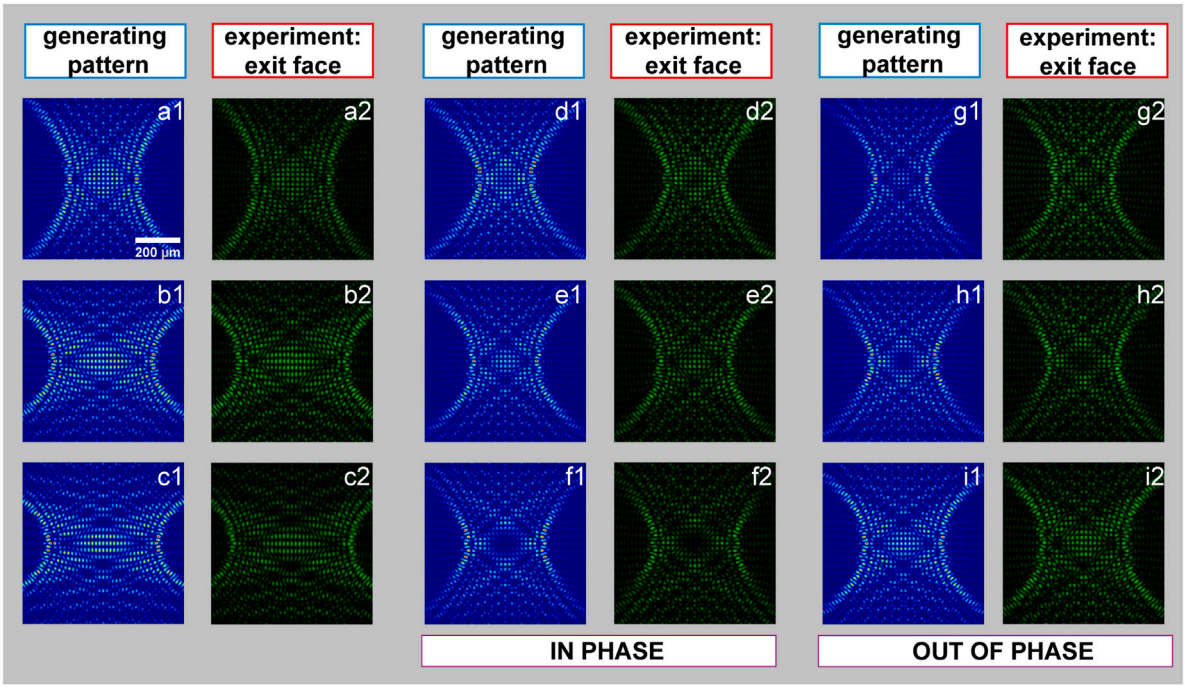


Fig. 5. Mutual influence of horizontal beam shift and opposite-sing parabolicities. (a)–(c) $d_x = 648$ μm, (a) $a_1 = 15, a_2 = -15$, (b) $a_1 = 20, a_2 = -20$, (c) $a_1 = 35, a_2 = -35$. (d)–(i) $a_1 = 25, a_2 = -25$; (d), (g) $d_x = 486$ μm, (e), (h) $d_x = 540$ μm, (f), (i) $d_x = 594$ μm. The third and the fourth columns show in-phase, and the fifth and the sixth columns out of phase beam configurations.

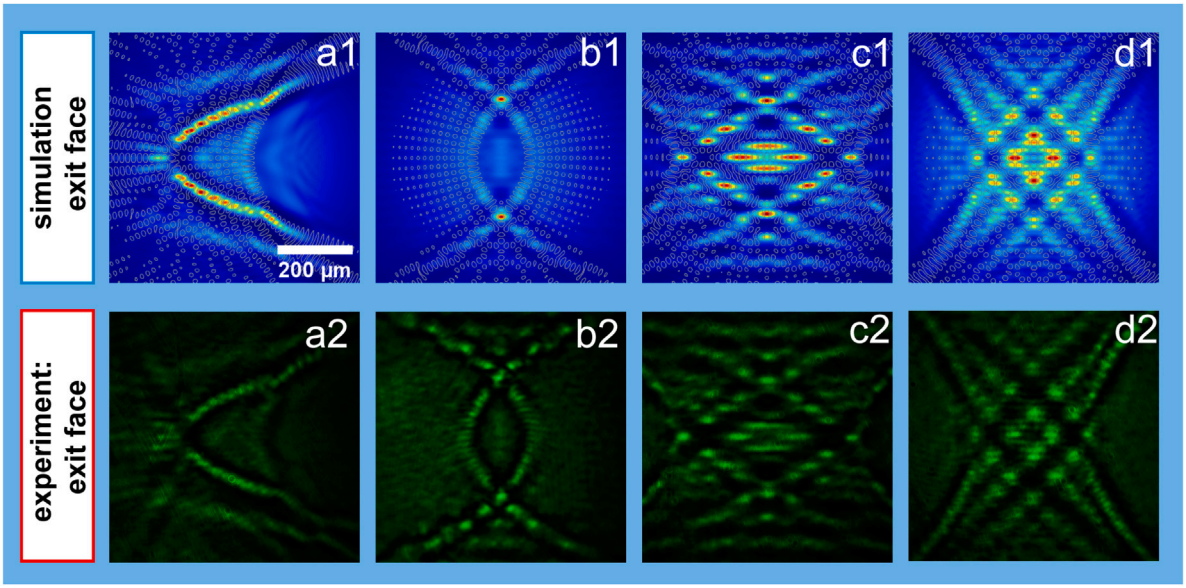


Fig. 6. Deterministic aperiodic photonic lattices (inscribed into the SBN crystal) existence and 2D nature verification by an extraordinarily polarized broad Gaussian beam probing. Intensity distributions of the probe beam at the exit face of the crystal were obtained numerically (the top row) and experimentally (the bottom row) for lattices given in (a) Fig. 3(a); (b) Fig. 4(c); (c) Fig. 5(c); and (d) Fig. 5(a). Contours in numerical results indicate waveguide position.

with distinct defects: dot or line shape defects and even macro defects. With such parabolic structures, one can generate various kinds of deterministic aperiodic photonic lattice edges characterized by higher or lower lattice strength regions that could be useful for surface state investigation. The lattice edge shapes and strengths can be managed by changing Weber beam parabolicities and their vertical shifts.

Keeping positive parabolicities ($a_1, a_2 > 0$ and $a_1 \neq a_2$) and $d_y = 0$, we study the interference of beams shifted along the x-axis in *in-phase* and π *out-of-phase* configurations (Fig. 3). The phase difference is equivalent to z-shift. All structures are symmetric under reflection over horizontal axes. With these interference patterns, it is possible to generate truncated deterministic aperiodic photonic lattices with different lattice edge shapes and strengths. Such structures possess distinct lattice regions of various shapes, with their transition lines that are also interesting for future investigation. Changing beam parabolicity, mutual distance, and phase relations allow one to continuously introduce the degree of asymmetry and defect sizes, shapes, and positions. By switching the phase configurations, it is possible to manage lattice strength along the edges, as well as alternate defect positions.

Next, we superimpose two Weber beams of the *same parabolicities* but of opposite signs and observe distinctive structures (Fig. 4(b),(c)) that are symmetric under reflection over both horizontal and vertical

axes. However, using *different parabolicities* of opposite signs, asymmetric intensity distributions are observed, mirror-symmetric to the x-direction (Fig. 4(a), (d)). These structures have lattice edges, characterized by higher lattice strength, that are not open as in previous cases but closed, generating macro defects — enclosed areas without lattice sites. By changing beam parabolicities, it is possible to separately control the curvature of macro defect sides separately and thus their size. One can see the regions of unchanged separate Weber beams and distinct defect types.

In Fig. 5(a)–(c), we present examples of Weber beams whose mutual distance is kept constant (with $d_y = 0$) and *opposite parabolicities* ($a_1 = -a_2$) take different values. Varying the parabolicity changes the distance between the left and right lattice edges. The central regions of the rhombic shape, with waveguide distribution resembling the periodic lattice, elongate along the x-axis with decreasing Weber beam parabolicity. That stretching of the rhombic contour results in redistribution of sites so that the number of horizontal lattice sites increases and the number of vertical sites decreases, with negligible effect on their mutual distances (period), but with individual waveguide shapes becoming more elliptical. Stretching of triangular shape regions above and below this region, where the distribution of waveguides resembles transitionally octagonal lattice, occurs similarly.

In Fig. 5(d)–(i), we show the effect of the relative phase (z-shift) of Weber beams with fixed parabolicities ($a_1 = 25$ and $a_2 = -25$) whose distance varies, keeping $d_y = 0$. Switching from in-phase (Fig. 5(d)–(f)) to out-of-phase (Fig. 5(g)–(i)) configurations leads to alternating regions of defect positions with lattice sites of higher and lower intensity. We can enrich the class of available complex patterns by manipulating the combination of parabolicities and x, y, and z shifts. Note that the middle part of all lattices in Fig. 5 has considerably higher lattice intensity interfacing with parabolically shaped regions without overlap and lower lattice intensity.

3.2. Plane-wave aperiodic deterministic 2D photonic lattice probing

Light structures, i.e., parabolic deterministic 2D aperiodic lattices, whose x–y plane cross-sections are shown in the previous section, were obtained in the air and the refractive medium — the SBN crystal. To verify their existence and 2D nature (refractive index modulation is the same at any x–y plane) within the crystal, we probe them with an extraordinarily polarized broad Gaussian beam. Fig. 6 presents numerical and experimental intensity distributions, according to the underlying refractive index modulation, at the exit face of the crystal, demonstrating that the incident broad beam was transmitted through the 2D aperiodic lattice written in the crystal. As the intensity is preferentially guided in the areas of higher refractive index, the agreement between the experimentally observed intensity distribution at the exit face of the crystal with the respective generating pattern confirms the accuracy of our optically induced lattices. Furthermore, the numerical predictions of probe beam propagation agree well with experimental results.

4. Conclusion

We have developed an approach for creating advanced, naturally truncated, deterministic aperiodic photonic lattices of parabolical geometry realized in SBN crystal in a one-pass experimental setup. Superimposing two non-diffracting Weber beams with different parabolicities, positions, and relative phases leads to transverse-invariant intensity distributions capable of inducing corresponding refractive index variations – lattices – in photosensitive media. Light propagation in such exotic structures, particularly the impact of boundaries, is still an unexplored topic that will thus be thoroughly investigated in linear and nonlinear regimes in future work. Randomization of these structures allows for an additional light control level, providing a step towards novel waveguiding applications and light routing approaches.

CRediT authorship contribution statement

Aleksandar Ž. Tomović: Writing – original draft, Methodology, Investigation. **Isidora J. Vlaović Mitić:** Visualization, Investigation, Formal analysis, Data curation. **Vladimir P. Jovanović:** Writing – review & editing, Validation, Investigation, Formal analysis. **Dejan V. Timotijević:** Writing – review & editing, Supervision, Software, Methodology, Conceptualization. **Dragana M. Jović Savić:** Writing – review & editing, Supervision, Funding acquisition, Conceptualization.

Declaration of competing interest

The authors declare no conflicts of interest.

Acknowledgments

The authors acknowledge funding provided by the Institute of Physics Belgrade and Institute for Multidisciplinary Research (IMSI), through the grants by the Ministry of Science, Technological Development and Innovations of the Republic of Serbia (IMSI contract no. 451-03-66/2024-03/200053) and by the Science Fund of the Republic of Serbia, GRANT No 7714356, IDEAS - CompsLight.

Data availability

Data will be made available on request.

References

[1] T. Schwartz, G. Bartal, S. Fishman, M. Segev, Transport and Anderson localization in disordered two-dimensional photonic lattices, Nature 446 (2007) 52–55.
[2] Z.V. Vardeny, A. Nahata, A. Agrawal, Optics of photonic quasicrystals, Nat. Photonics 7 (2013) 177–187.
[3] D. Shechtman, I. Blech, D. Gratias, J.W. Cahn, Metallic phase with long-range orientational order and no translational symmetry, Phys. Rev. Lett. 53 (1984) 1951–1953.
[4] D. Levine, P.J. Steinhardt, Quasicrystals: A new class of ordered structures, Phys. Rev. Lett. 53 (1984) 2477–2480.
[5] B. Freedman, G. Bartal, M. Segev, R. Lifshitz, D.N. Christodoulides, J. Fleisher, Wave and defect dynamics in nonlinear photonic quasicrystals, Nature 440 (2006) 1166–1169.
[6] L. Dal Negro, S.V. Boriskina, Deterministic aperiodic nanostructures for photonics and plasmonics applications, Laser Photonics Rev. 6 (2012) 178–218.
[7] M. Baake, U. Grimm, Mathematical diffraction of aperiodic structures, Chem. Soc. Rev. 41 (2012) 6821–6843.
[8] H. Hiramoto, M. Kohmoto, Electronic spectral and wavefunction properties of one-dimensional quasiperiodic systems: a scaling approach, Internat. J. Modern Phys. B 6 (1992) 281–320.
[9] E. Maciá, The role of aperiodic order in science and technology, Rep. Progr. Phys. 69 (2006) 397–441.
[10] G. Gumbs, M.K. Ali, Dynamical maps, Cantor spectra, and localization for Fibonacci and related quasiperiodic lattices, Phys. Rev. Lett. 60 (1988) 1081–1084.
[11] R. Lifshitz, The square Fibonacci tiling, J. Alloys Compd. 342 (2002) 186–190.
[12] S.V. Boriskina, A. Gopinath, L. Dal Negro, Optical gap formation and localization properties of optical modes in deterministic aperiodic photonic structures, Opt. Express 16 (2008) 18813–18826.
[13] M. Boguslawski, N.M. Lučić, F. Diebel, D.V. Timotijević, C. Denz, D.M.J. Savić, Light localization in optically induced deterministic aperiodic Fibonacci lattices, Optica 3 (2016) 711–717.
[14] I.A. Glukhov, Y.S. Dadoenkova, F.F.L. Bentivegna, S.G. Moiseev, Deterministic aperiodic photonic crystal with a 2D array of metallic nanoparticles as polarization-sensitive dichroic filter, J. Appl. Phys. 128 (2020) 053101.
[15] Q.-D. Ou, L. Zhou, Y.-Q. Li, S. Shen, J.-D. Chen, C. Li, Q.-K. Wang, S.-T. Lee, J.-X. Tang, Extremely efficient white organic light-emitting diodes for general lighting, Adv. Funct. Mater. 24 (2014) 7249–7256.
[16] J. Durnin, J.J. Miceli, Jr., J.H. Eberly, Diffraction-free beams, Phys. Rev. Lett. 58 (1987) 1499–1501.
[17] J.C. Gutiérrez-Vega, M.D. Iturbe-Castillo, S. Chávez-Cerda, Alternative formulation for invariant optical fields: Mathieu beams, Opt. Lett. 25 (2000) 1493–1495.
[18] M.A. Bandres, J.C. Gutiérrez-Vega, S. Chávez-Cerda, Parabolic nondiffracting optical wave fields, Opt. Lett. 29 (2004) 44–46.

[19] P. Rose, M. Boguslawski, C. Denz, Nonlinear lattice structures based on families of complex nondiffracting beams, New J. Phys. 14 (2012) 033018.
[20] M. Woerdemann, C. Alpmann, M. Esseling, C. Denz, Advanced optical trapping by complex beam shaping, Laser Photonics Rev. 7 (2013) 839–854.
[21] C.-W. Qiu, D. Palima, A. Novitsky, D. Gao, W. Ding, S.V. Zhukovsky, J. Gluckstad, Engineering light-matter interaction for emerging optical manipulation applications, Nanophotonics 3 (2014) 181–201.
[22] J.M. Vasiljević, A. Zannotti, D.V. Timotijević, C. Denz, D.M.J. Savić, Creating aperiodic photonic structures by synthesized Mathieu-Gauss beams, Phys. Rev. A 96 (2017) 023840.
[23] J.M. Vasiljević, A. Zannotti, D.V. Timotijević, C. Denz, D.M.J. Savić, Light propagation in aperiodic photonic lattices created by synthesized Mathieu–Gauss beams, Appl. Phys. Lett. 117 (2020) 041102.
[24] J.M. Vasiljević, A. Zannotti, D.V. Timotijević, C. Denz, D.M.J. Savić, Light transport and localization in disordered aperiodic Mathieu lattices, Opt. Lett. 47 (2022) 702–705.
[25] W. Liu, J. Gao, X. Yang, Optical transportation of micro-particles by non-diffracting Weber beams, J. Opt. 20 (2018) 125401.
[26] Y.S. Kivshar, Nonlinear tamm states and surface effects in periodic photonic structures, Laser Phys. Lett. 5 (2008) 703.
[27] S. Suntsov, K.G. Makris, G.A. Siviloglou, R. Iwanow, R. Schiek, D.N. Christodoulides, G.I. Stegeman, R. Morandotti, H. Yang, G. Salamo, M. Volatier, V. Aimez, R. Arès, M. Sorel, Y. Min, W. Sohler, X. Wang, A. Bezryadina, Z. Chen, Observation of one- and two-dimensional discrete surface spatial solitons, J. Nonlinear Opt. Phys. Mater. 16 (2007) 401–426.
[28] K.G. Makris, S. Suntsov, D.N. Christodoulides, G.I. Stegeman, A. Hache, Discrete surface solitons, Opt. Lett. 30 (2005) 2466–2468.
[29] C.R. Rosberg, D.N. Neshev, W. Krolikowski, A. Mitchell, R.A. Vicencio, M.I. Molina, Y.S. Kivshar, Observation of surface gap solitons in semi-infinite waveguide arrays, Phys. Rev. Lett. 97 (2006) 083901.
[30] X. Wang, A. Bezryadina, Z. Chen, K.G. Makris, D.N. Christodoulides, G.I. Stegeman, Observation of two-dimensional surface solitons, Phys. Rev. Lett. 98 (2007) 123903.
[31] U. Peschel, R. Morandotti, J.S. Aitchison, H.S. Eisenberg, Y. Silberberg, Nonlinearly induced escape from a defect state in waveguide arrays, Appl. Phys. Lett. 75 (1999) 1348–1350.
[32] H. Trompeter, U. Peschel, T. Pertsch, F. Lederer, U. Streppel, D. Michaelis, A. Bräuer, Tailoring guided modes in wave- guide arrays, Opt. Express 11 (2003) 3404–3411.
[33] E. Gavartin, R. Braive, I. Sagnes, O. Arcizet, A. Beveratos, T.J. Kippenberg, I. Robert-Philip, Optomechanical coupling in a two-dimensional photonic crystal defect cavity, Phys. Rev. Lett. 106 (2011) 203902.
[34] A.A. Zozulya, D.Z. Anderson, Propagation of an optical beam in a photorefractive medium in the presence of a photogalvanic nonlinearity or an externally applied electric field, Phys. Rev. A 51 (1995) 1520–1531.
[35] D.V. Timotijević, J.M. Vasiljević, D.M.J. Savić, Numerical methods for generation and characterization of disordered aperiodic photonic lattices, Opt. Express 30 (2022) 7210–7224.

Book of abstracts



PHOTONICA 2025

X International School and Conference on Photonics

25 - 29 August 2025

Belgrade, Serbia

Editors

Mihailo Rabasović, Uroš Ralević, Marina Lekić, Aleksandar Krmpot
Institute of Physics Belgrade, Serbia

Belgrade, 2025

Deterministic aperiodic lattices generation with Weber beams

I. J. Vlaović Mitić[1], A. Ž. Tomović[2], V. P. Jovanović[2], D. V. Timotijević[2], and D. M. Jović Savić[1]
[1]*Institute of Physics, University of Belgrade, P.O. Box 68, 11001 Belgrade, Serbia*
[2]*Institute for Multidisciplinary Research, University of Belgrade, Kneza Višeslava 1, 11030, Belgrade, Serbia*
e-mail: isidora@ipb.ac.rs

Light propagation in periodic photonic structures is controlled by spatial and temporal photonic band gaps; however, the manipulation of light in deterministic aperiodic and complex photonic structures remains poorly understood and unexplored for practical applications [1]. Nondiffracting beams, characterized by their propagation-invariant intensity profiles, are well-suited for creating photonic lattices in photosensitive media [2,3]. A method for generating deterministic aperiodic photonic lattices through the interference of two coherent Weber beams is presented [4]. These patterns are used to induce refractive index modulations in a photorefractive SBN crystal via single-pass optical induction. Various two-dimensional truncated aperiodic lattices were realized by adjusting the beams' parabolicities, relative phases, orientations, and spatial displacements. The resulting structures exhibit asymmetric domains, localized and extended defects, and enclosed macro-defect regions, offering diverse configurations suitable for studying wave localization, photonic surface states, and light manipulation in aperiodic systems. The formation and properties of the induced lattices were predicted through numerical simulations based on an anisotropic model. Their existence and guiding behavior were experimentally confirmed by probing with an extraordinarily polarized Gaussian beam. This approach provides a robust and versatile platform for the fabrication of deterministic aperiodic photonic media using structured light, with potential applications in integrated photonic devices, nonlinear optics, and topological light control.

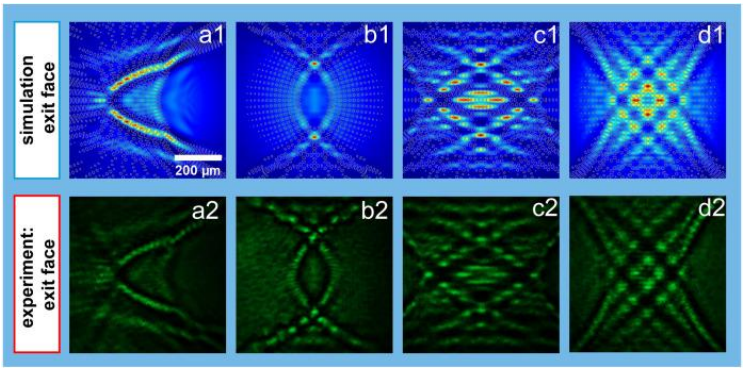


Figure 1. Verification of deterministic aperiodic photonic lattices inscribed in a photorefractive SBN crystal through probe beam propagation. Intensity distributions of the probe beam at the exit face of the crystal obtained numerically (the top row) and experimentally (the bottom row). Contours in numerical results indicate waveguide position.

REFERENCES

[1] Z. V. Vardeny, A. Nahata, A. Agrawal, Nat. Photonics 7, 177 (2013).
[2] M.A. Bandres, J.C. Gutiérrez-Vega, S. Chávez-Cerda, Opt. Lett. 29, 44–46 (2004).
[3] J. M. Vasiljević, A. Zannotti, D. V. Timotijević, C. Denz, D. M. Jović. Savić, Phys. Rev. A 96, 023840 (2017).
[4] A. Ž. Tomović, I. J. Vlaović Mitić, V. P. Jovanović, D. V. Timotijević, D. M. Jović Savić, Optical Materials 157, 116334 (2024).

ORCID: I.V. M. 0009-0003-1794-4278, A.T. 0000-0001-5972-6760, V.J. 0000-0001-6640-4575, D.T. 0000-0003-4538-3140, D.J.S, 0000-0002-1081-0141